

Airfoil Journal Bearing – The Road to a Million Start Stops

Hans Gangwar
 Research Engineer
 Fuel Cell Systems Research
 Ford Motor Company
 1201 Village Rd.
 Dearborn, MI 48124
 hgangwar@ford.com

Rob Anderson
 Senior Technologist
 Vortech Engineering, LLC
 1650 Pacific Avenue
 Oxnard, CA 93033
 randerson@vortechsuperchargers.com

Kyeong-Su Kim
 Director
 Turbo Energy R&D
 Neuros LTD
 Tamnip-dong 825 Yuseong-gu
 Daejeon, Korea
 mcpie@neuros.co.kr

ABSTRACT

Airfoil bearings have been limited by the number of start-stops due to mechanical wearout of coating(s) at low, pre lift-off speeds. However, automotive hybrid electric vehicle applications require 1 million start-stops or more. This same level of start-stops is also required for hydrogen PEM fuel cell vehicles. In this investigation, a test regime is developed to stress the failure mode of airfoil bearings caused by start-stops and conceive improvements to meet the requirement. A complete electronic air cathode compressor (electronic supercharger) assembly is tested, with two Ø25mm journal airfoil bearings. The top foils have 34µm of surface PTFE coating. After 50,000 start-stops, the coating is worn through. Next an improved design is tested, which has modified coating on the bearing journal surfaces. These bearings are examined roughly every 250,000 start-stops. After 1 million start-stops, the coating has worn 5µm. The data is further analyzed using statistical reliability techniques. These predict an L_{10} of 8.7 million start-stops. The cost of modifying the treatment to extend the lifetime to 1 million start-stops is a 1% price change (off a base of \$20). This shows the technology is feasible for automotive usage.

INTRODUCTION

Even with the advances in hydrogen technology in the last decade, there are still many challenges to overcome before fuel cell vehicles can compete in the market with current vehicle technology. The cost and durability of the fuel cell system are the most significant challenges. In order to make the electronic supercharger (ESC) in the fuel cell commercially viable, a direct coupled centrifugal device provides the smallest (for both mass and volume) device at the lowest cost. The power density and specific power comparisons for three viable compressor technologies are shown in Figure 1, and include the power electronics necessary for driving the compressor. For the centrifugal technology, power density (power per unit volume) is 1.13 kW/L,

while specific power (power per unit mass) is 0.7 kW/kg. This performance meets US Department of Energy targets for the automotive fuel cell air cathode compressor [1]. However, to achieve this superior performance, the centrifugal impeller must spin upwards of 100,000 rpm in order to efficiently produce 2.5 bar pressure at 325 kg/hr airflow. At these speeds, bearing design is challenging.

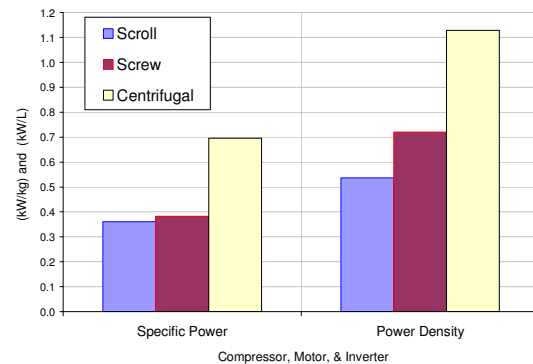


Figure 1. Specific Power (kW/kg) and Power Density (kW/L) for candidate compressor technologies, taken at 2.5 PR and 325kg/hr air flow

The lifetime of airfoil bearings for high speed continuous operation is virtually infinite. This has been proven in Air Cycle Machines (ACM). ACMs are used in environmental cooling systems in aircraft. Virtually every ACM since 1990 has used airfoil bearings. For example, the airfoil bearing used in the Boeing 747 air cycle machine has demonstrated a MTBF (mean time between failure) in excess of 100,000 hours [2], [3]. For high speed (75,000 rpm or greater) operation, the lifetime of the closest competitor technology, ceramic ball anti friction bearings, is less than 3,000 hours [4]. One limiting factor for automotive use of airfoil bearings has been the number of start-up cycles. The concern has been that while airfoil bearings have enjoyed considerable commercial success in aviation and various industrial applications where start-stops on the order of 50,000 cycles has been the de facto standard, automotive

start-stop requirements are an order of magnitude greater than this. For long life performance, anti friction/wear coatings on foils and/or mating journals are necessary to primarily negate the effects of the “in-contact” wear experienced during start-stop events [5]. However, research on improving the coating for airfoil bearings has been oriented more towards extending the max temperature capability of the bearings [6] than on increasing the number of start-stops. For automotive fuel cell applications, power compartment operating temperatures of up to 100°C are considered the upper limit, and this is well within the capable range of low-cost PTFE materials. Thus, there is little benefit to use of high temperature coatings as the compressor device would typically not be exposed to such extreme thermal environments. One might ask: “So, what is the start stop requirement for a hybrid vehicle?” Referring to the National Renewable Energy Laboratory, the number of start-stops for a 12V micro-hybrid vehicle is 750,000 cycles [7]. Currently, however, major automotive company design requirements exceed 1 million cycles [8]. Therefore, a means of testing to 1 million start-stops has to be determined, and a feasible bearing system design provided. Start-stop testing is to be conducted on airfoil bearings in an electronic supercharger shown in Figure 2. To validate the test protocol, a baseline bearing set is first tested. Then an improved bearing set is tested to demonstrate enhanced start-stop durability.



Figure 2. Electronic Supercharger (ESC), Integral Motor/Compressor System

BEARING TECHNOLOGY

In order to accommodate an automotive environment, the airfoil journal bearings (within a centrifugal compressor and motor) are modified to withstand 1 million start-stops. The rotating journal is treated with a titanium nitride (TiN) coating, followed by a

molybdenum disulfide (MoS_2) treatment. The stationary bearing top foil is treated with a filled PTFE (polytetrafluoroethylene or Teflon) coating, with higher shear strength. A pair of Ø25mm by 30mm length (effective bearing length) journals are used to support the rotor system, each located on either end of a permanent magnet (PM) rotor. These are referred to as “fore” and “aft” for the purposes of discussion. The system also incorporates a pair of airfoil thrust pads, and numerous other components such as motor stator, motor cooling jacket, impeller, volute, and main housing components. But because this study is primarily focused on the life/wear-out performance of the journal bearing top foil, discussion is limited to these components in this presentation.

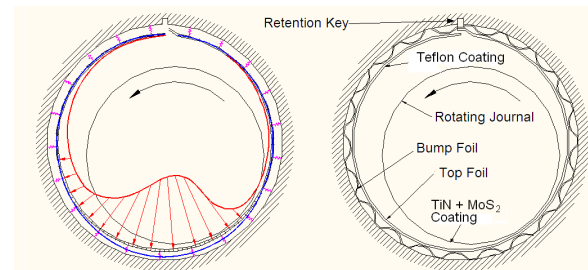


Figure 3. Airfoil Bearings

A cross sectional schematic of an airfoil bearing is shown in Figure 3. The right side of the figure shows generally the different parts of the bearing used in this study – top foil, bump foil, rotating journal, location of PTFE coating, and retention key. The bearings used in this study are considered “GEN-II”, meaning, they employ a segmented bump foil which bears in the housing bore, and supports a pair of foils, the first top foil being prepared with the PTFE-based coating [9] [10]. Details of the bearings and other system parameters are summarized in Table 1. The rotor system of the ESC is depicted in Figure 4.

The test bearing systems are further characterized by the specific construction of the journals against which the foils will operate. For a permanent magnet machine with the journals in direct contact with the permanent magnet rotor, it is beneficial to construct the journals from non ferromagnetic material. Further, it is common for the journals to be of low surface roughness and high hardness, with the latter property in order to be resistant to potential abrasive wear. Meeting all of these criteria compounded with the need for low-cost requirements of typical automotive use is a challenge. The ESC, therefore, employs a journal design of low-cost AISI 304, which is further finished by an abrasive “peening”

process to attain a very smooth, quasi-cased surface finish (Ra) of .05 – .10 μ m. This constitutes the “Baseline” configuration. The “Improved” design modifies the Journal surfaces by applying additional low-cost treatments: a titanium-nitride coating of approximately 2 – 5 μ m thickness is applied for the anti-wear properties, and then one last treatment of molybdenum disulfide (MoS₂) coating of approximately 0.5 μ m for added anti-friction performance. The Improved system, then, results in anti-friction property treatments applied to both journal (MoS₂) and top foil (PTFE).

Table 1. Summary of ESC Bearing/Rotor System Parameters

Item	Dimension	Material
Bearing Journal \varnothing	25mm	AISI 304
Bearing Journal Length	30mm	-
Journal Treatment, Baseline	.05-.10 μ m Ra	AISI 304
Journal Treatment, Improved	2-5 μ m + .5 μ m	TiN +MoS ₂
Housing Bore \varnothing	26.67mm	Al 6061
Bore Treatment	25 μ m	Type III Anodize
Top Foil Th.	87 μ m	IN 718
Top Foil Treatment	34 μ m	Filled PTFE
2 nd Foil Th.	87 μ m	IN 718
Rotor Mass	942 g	-
Bearing Span	90mm	Brg C/L – C/L

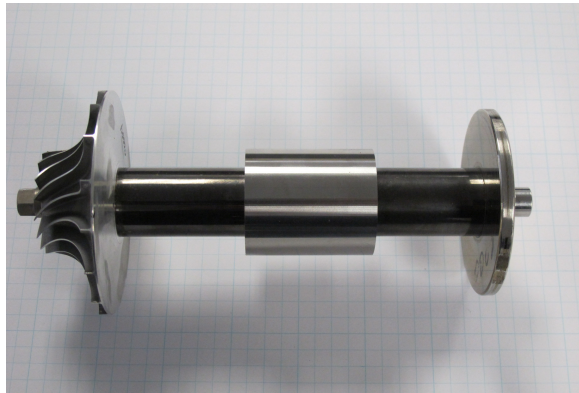


Figure 4. Assembled ESC Rotor System showing impeller (Left), fore/aft bearing journals, PM rotor, and thrust disk (Right).

TEST STAND LAYOUT

As shown in Figure 5, the test stand is plumbed according to SAE standards [11]. Two pressure sensors clocked 90 degrees and 75mm apart are installed on the inlet and outlet pipes of the air compressor. Two temperature sensors clocked 90 degrees and 75mm apart are also installed on the inlet and outlet pipes of the air compressor. The approximately 75mm pipe diameter is chosen on both inlet and outlet pipes so stagnation conditions are measured (flow velocity contribution of dynamic pressure is minimal). Also according to [11], the transition from 75mm diameter ducting to the inlet and outlet of the compressor is within an effective length of 1.5 x diameters. And sensors are located at least 150mm away from the transitions.

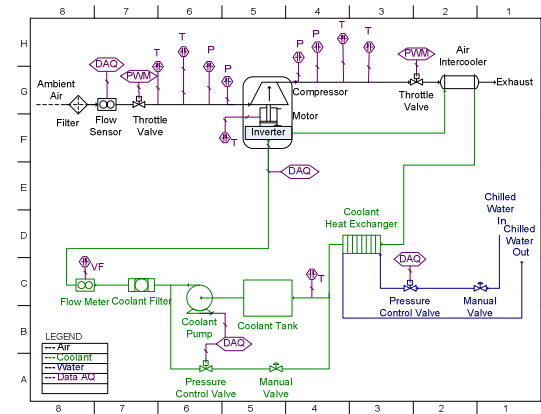


Figure 5. Process diagram/schematic of test stand setup and operation

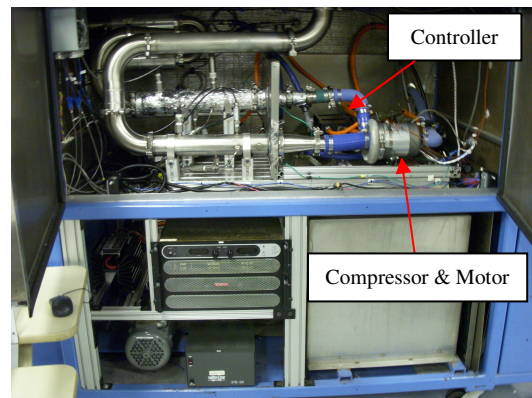


Figure 6. Test stand front view

The test stand is shown pictorially in Figure 6. The compressor is placed inside an enclosed test chamber for safety. The compressor and motor are shown on the right, inside the test chamber, with the black

controller module (inverter) directly behind it. The large stainless steel box below the compressor is the water ethylene glycol mixture reservoir (for cooling of the controller / motor). Next to the reservoir is the high voltage DC power supply. A power supply converts 480VAC from the wall to 325V DC supply for the electronic supercharger. Next to the power supply (on left) is a large diode to prevent damage to the power supply from any potential reversals. Below the power supply is the coolant pump. Test stand software enabled the automatic running of a test profile (24 hours, 7 days, 52 weeks) as long as 480VAC power is provided. A PC-based controller and data acquisition system controls the actuators and records the data.

START STOP PROFILE

When at operational speeds, the bearings operate with the journals riding on a thin film of air. Wear occurs on airfoil bearings during lift off and touch down. The term “lift-off” refers to the journal transitioning from contacting the foil surface while rotating to instead riding on a thin film of air. The term “touch-down” refers to the opposite phenomenon – the journal transitions from riding on a thin film of air to instead contacting the foil surface while rotating. Therefore to stress the failure mechanism for start-stop cycles, cycling is conducted for lift-off and touch-down, and repeated. The time required for touch down and ultimately zero rotor speed depends on the initial rotational speed, rotating inertia, aerodynamic drag, and the frictional torque after touchdown. In the case of the Electronic Supercharger (ESC) the minimum “idle” speed is 10,000rpm (i.e., rotor system is “airborne” and stable with speed margin) and the coast down time is about 8 seconds from 10,000rpm. Previous laboratory tests have consistently shown the touchdown speed of the ESC is in the range of 4,000 – 5,000 rpm, as indicated by a noticeable change in the slope of the rotor speed vs. time coast down curve.

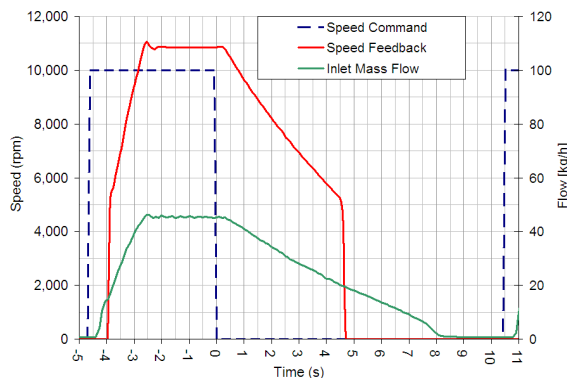


Figure 7. 15s Start Stop profile

A 15s repetitive cycle is defined. An up transient (followed by a down transient) are used to “wear” the bearings. Referring to Figure 7, the speed command is shown in blue, the speed feedback in red, and the inlet air mass flow in green. Inspecting the figure, at time -4.5s, the rotor is stopped and the speed is at 0 rpm. An up transient step function then occurs, with a speed command of 10,000 rpm which is held between [-4.5, 0]s. Now the down transient is lined up with 0s in the figure. From [0, 10.5]s the speed is commanded to 0rpm. During these tests, the resolver could not properly detect speeds below 5000rpm. Therefore, in order to ensure the rotor has fully come to rest, system air mass flow is also used as an indication (but not as a determination of lift-off speed). This testing is conducted as part of a rotor assembly in a fully functioning electronic supercharger (motor and compressor assembly with controller). It is not meant to just validate the bearings, but the bearings in a production assembled product environment.

RESULTS, BASELINE

As mentioned earlier, a baseline bearing system validated the test protocol. It is important to confirm that the test cycle is stressing the known failure mode. Referring to Figure 8, the baseline system after 50,000 start-stops shows the top foil has experienced substantial wear-through of the PTFE coating. The foil in this region is now experiencing metal-to-metal contact during start-stop operation. Here "a" indicates the foil retaining tab, "1" indicates where the rotor touches down on a stop (consistently the same angle) and "2" indicates where the rotor lifts off during a start (feathering as the location changes and the journal rotating axis shifts). Although the machine can still start up and function, continued start-stop events will inevitably lead to highly accelerated wear of both the foil and mating journal, and rapid wear-out of the entire system. Having accomplished only 1/20th the desired start-stop life, the baseline system does not meet requirements.

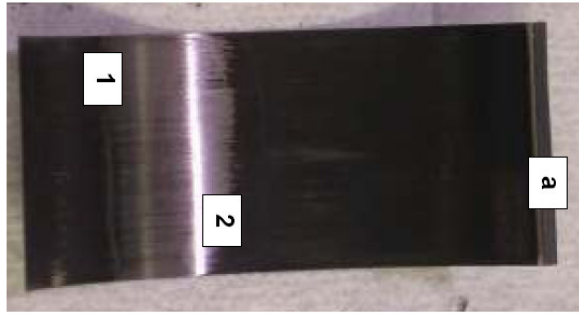


Figure 8. Top foil, baseline system, after 50k start-stops

Therefore the 15 second profile shows the bearing cycling has truly worn through the PTFE coating, exposing the base metal. So, after 50,000 start-stops, the top foil is considered to be at the end of life. This validates the test cycle.

RESULTS, IMPROVED

Next an improved design is tested. Since the lifetime of the improved design is for 1 million start-stops, wear needs to be measured periodically. This periodic inspection of the bearings will allow a failure model to be generated.

Aside from the initial new bearing inspection, intermediate teardown and inspections occurs at 125k start-stops, 264k start-stops, 392k starts stops, 800k start-stops, and 1.01M start-stops. The thickness of the top airfoil is measured and then the electronic supercharger is reassembled. The top foils can be expected to wear, even if slightly, over this many start-stop cycles. This will reduce the overall thickness of the foils, which in turn may affect the internal clearance of the bearing, and hence operating characteristic of the machine over its speed range of interest. Thus after each re-build, the ESC was confirmed operational on the stand by running up to a maximum 90krpm, with no anomalies observed. Once proper “as new” operation is confirmed, the start-stop cycling is then resumed.

A handheld digital Precision Micrometer is used to measure total thickness of the top foil. The tool has a resolution of $1\mu\text{m}$ [.00005in]. Bearing inspection is conducted by three operators at each inspection, with each taking a minimum of three measurements.¹ All

¹ Attempts were made to measure the thickness more accurately using an electron microscope, ultrasound, and eddy current techniques (non destructive). Unfortunately the ultrasound and microscope were not able to discern the PTFE coating from the IN 718

measurements are conducted at a consistent, stabilized 21°C ambient. Selection of the measurement location is shown in Figure 9 at the red dots, with two middle location points chosen. Baseline bearing testing indicated this location is at or near the area of most wear. By measuring at the top and bottom edges, any tilt in the rotor assembly during lift off and touch down is accounted for. Additional locations are also measured, however those results do not provide any significantly different wear trends, i.e., results were at or less than the severity of wear found in the middle, so are not presented.



Figure 9. Top Foil overall thickness measurement (left) and measurement locations (right)

Gage R&R

A gage repeatability and reproducibility (R&R) study is necessary to validate the wear measurement technique. A total of 72 measurements are conducted by 3 operators on 8 samples with 3 replicates. The 8 samples consist of 4 at beginning of life and 4 at end of life. The End of Life (EOL) thickness is after the PTFE coating has completely worn off the foil, where the foil backer thickness is $87\mu\text{m}$. The Beginning of Life (BOL) thickness is a new foil with PTFE coating of $34\mu\text{m}$ applied; total thickness being $121\mu\text{m}$. BOL and EOL parts are used because the purpose here is to understand the degradation over the life, and the gage's ability to measure progressive change. In this case, a single measurement point is selected, directly in the middle of the bearing. The Gage resolution is determined to be $\pm 1.75\mu\text{m}$ (i.e., Std Dev for Total Gage R&R) even though the micrometer instrument itself has a resolution of $1\mu\text{m}$.

The upper left graph in Figure 10 shows study variation constitutes less than 10% of the variation in the measurement. When BOL and EOL parts are compared, the individual operator is able to measure the same value consistently (repeatable) and different operators measure the same part consistently

foil backer. The eddy current produced results with the same standard deviation as the micrometer, but required additional care in calibrating (new part mean $30.2\mu\text{m}$ instead of $34\mu\text{m}$).

(reproducible). The lower left graph in Figure 10 shows the means of operators' measurements are virtually identical when compared to the spread of individual data points. The middle left graph in Figure 10 as well as Figure 11 show there are no plateaus per operator or per part, so the gage has enough resolution. However Operator A had more range variation than Operators B and C.

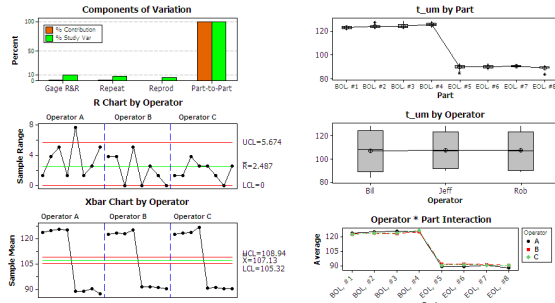


Figure 10. Gage R&R Graphical Results

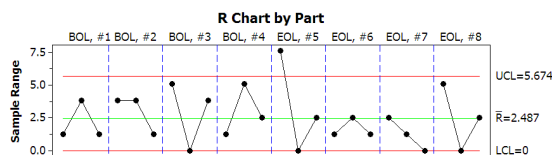


Figure 11. Range Chart by Part

Test Duration

This improved design is run for 1,013,000 start-stops. The run chart in Figure 12 shows the cumulative test duration conducted over almost 9 months. The test encompassed a total 4,250 hours of operational time. Every 625 hours equals 150,000 start-stops based on a 15s profile. As can be seen in the plot, the start stop cycles and the run time are line on line.

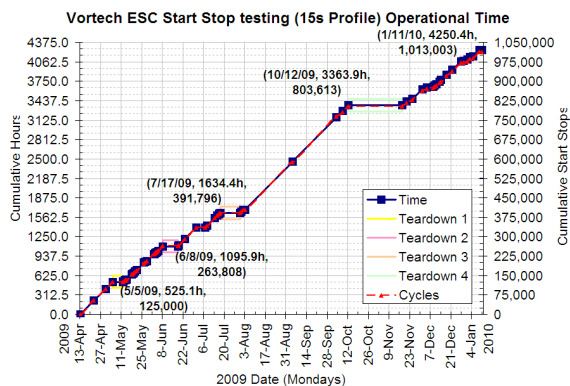


Figure 12. Start-stop run chart

Examining the speed feedback in Figure 14, the rotor speed consistently achieves 11,000 rpm. The spike

which occurs when the speed is first commanded from 0 to 10krpm is the result of electromagnetic interference (noise creating a false reading). The recording device thinks there is a Pulse Width Modulation signal at 100% duty cycle. This is from the start-up strategy to begin rotating the motor without knowing the actual position of the rotor – there is larger electromagnetic interference until the rotor begins rotating in synch with the stator phases.

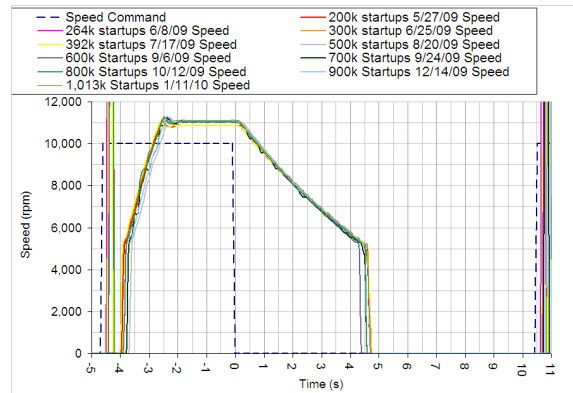


Figure 13. 15s start-stop profile; speed

The corresponding mass flow is plotted in Figure 14. There is a change in the idle flow after 800,000 start ups. This is because the mass flow sensors have been switched and a calibration offset of 10kg/h appears with the new sensors. The change in flow is the important measurement here, so a complete stop of the rotor can be detected.

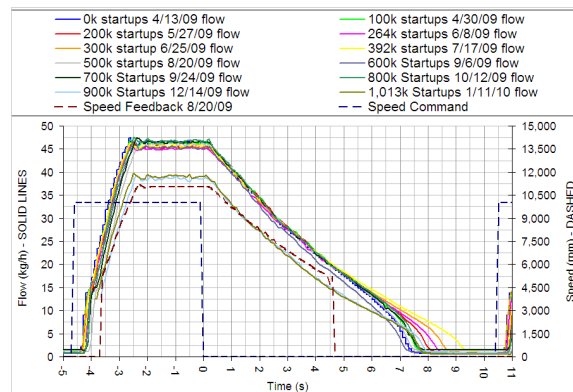


Figure 14. 15s Start-stop profile; air mass flow

Continuous Monitoring

Continuous monitoring is provided by an automatic data acquisition system. Speed command, resultant (feedback) speed, exhaust mass airflow, and motor power are the relevant data subgroups within the entire data group, which are acquired at 0.1s

intervals.² From this data, processed terms are collected for each validated start-stop recorded. This is important to track and show the bearings had actually lifted off and touched down 1,013,000 times. There is less than a 1% start-stop difference between data acquisition recorded events and actual commanded cycles. This is the reason the bearings are run for 1.3% margin over 1 million start-stops. Examining the processed data, there are some interesting effects in the stop time. Stop time is defined as the time to 95% decay – or when the air mass flow first records less than 2kg/h. The mass flow is selected as the trigger since speed feedback is only resolvable above 5,000rpm. The “stop” mass flow is the average mass flow during the last 1s of the OFF time in the profile. It should be noted that the mass airflow sensor used has a minimum value which is approximately 0.8 kg/h. As shown in Figure 15, the stop time is affected by stopping the test for a period of time. Each spike down towards 0 seconds is the performance after the unit had either been torn down or testing is temporarily interrupted for other reasons (loss of power, test stand work, revisions to control software, etc.). These spikes are indicated by a red arrow. The interruptions are clearly seen in Figure 16, where the post processed data is graphed by date.

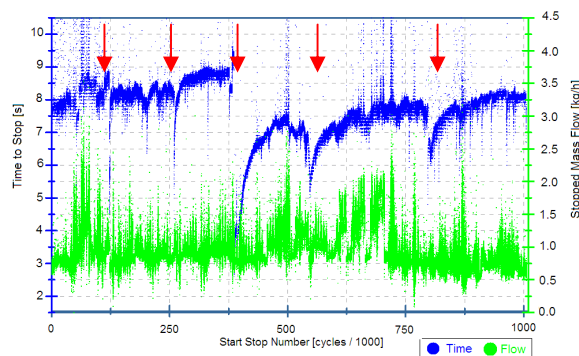


Figure 15. Stop time and flow by Run

Analysis of the post processed data shows there are no trends to indicate degradation over time. The data does show a slight dip in running average after the 392k teardown for stop time. Referring to Figure 15, because of this noted shift of the running average seen at 392k in the stop time, the decision is made to run cycling from 392k to 800k before a fourth teardown. In fact, between the 404k and 800k segment, there are two continuous blocks of 180k

² Acquiring just those five channels (includes timestamp) for 4,250.4 hours of operation at 0.1 sampling = 765 million individual data points, or 168 million data sets. This is why the data must be post processed, as this in its raw form is unmanageable.

cycles (as well as two 20k blocks). Pauses in the cycling are caused by a memory cache fault which lasts less than 2 minutes. For example, there is an interruption roughly at 550k start-stops (i.e. see the sudden dip towards 0 kg/h on stop time graph in Figure 15).

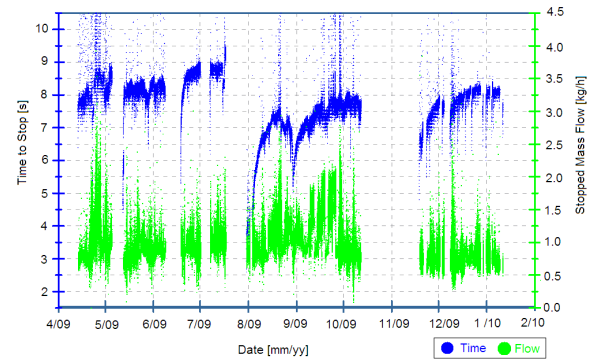


Figure 16. Stop time and flow by Date

Wear Measurement Results

For the improved design, testing is conducted for 1,013,000 start-stops. After 125,000 start-stops (3 weeks of 24 hour, 7 days a week cycling) the test is stopped with a subsequent teardown and bearing inspection (which includes thickness measurement). Inspection determined the bearings are in pristine condition and could last a much longer time. The test is repeated with a stop at 264,000 cycles, then at 392,000 cycles, then at 804,000 cycles, and finally at 1,013,000 cycles.

The measurement results are shown in Table 2, pictures of the airfoils are shown in Figure 17, and pictures of the journals in Figure 18. Reflections are circled in red on the pictures; all bearings remained completely coated with PTFE and are black in color

Table 2. Measured Thickness, Journal Top Foils

Start Stops Number	Time	Edge location	Fore Bearing			Aft Bearing		
			mean	St.Dev	Delta	mean	St.Dev	Delta
0	0	Top	122.6	16.6	0.0	123.5	1.1	0.0
		Bottom	123.0	1.2	0.0	123.5	1.1	0.0
125,000	525	Top	123.8	2.7	1.3	119.4	3.6	-4.1
		Bottom	120.7	1.8	-2.3	121.3	2.7	-2.2
263,808	1096	Top	122.6	4.5	0.0	121.3	2.7	-2.2
		Bottom	120.7	0.0	-2.3	121.3	1.9	-2.2
391,796	1634	Top	122.6	0.9	0.0	118.7	2.7	-4.8
		Bottom	120.7	1.8	-2.3	120.7	3.6	-2.9
803,613	3364	Top	119.8	4.8	-2.8	116.2	0.9	-7.3
		Bottom	118.7	0.9	-4.2	119.4	3.6	-4.1
1,013,003	4250	Top	118.7	2.7	-3.8	114.9	2.7	-8.6
		Bottom	119.4	0.0	-3.6	119.4	0.0	-4.1
cycles hours			µm	µm	µm	µm	µm	µm

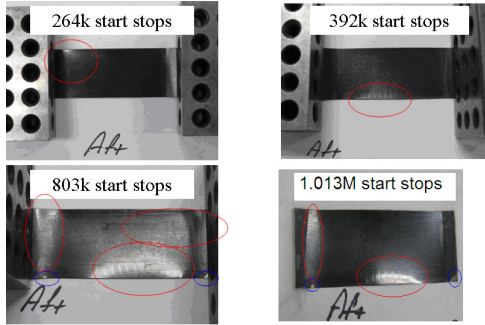


Figure 17. Aft Top Foil, Progressive Wear

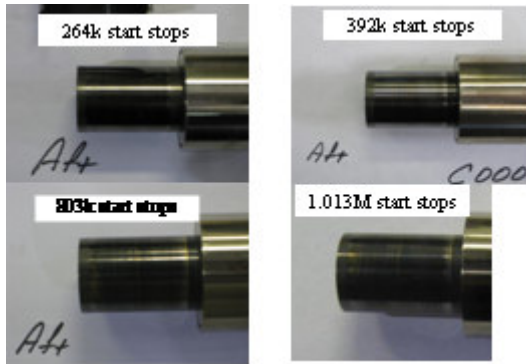


Figure 18. Aft Journal, Progressive Wear

does the wear. In other words, there is not perfectly uniform coating thickness on a new foil, nor is there perfectly uniform wear across the entire foil surface. Therefore, the foils will likely see some "breakthru" to bare metal at some localized zone long before the remaining PTFE goes away. At that point, the foil and journal could experience rapidly increasing wear over relatively few cycles, owing to rapidly expanding areas of metal-to-metal contact. Therefore, a conservative assessment of "EOL" is established, even if arbitrarily, where two-thirds of the PTFE has worn away at the measurement location. Using this criteria, the PTFE would be down to about 12.3 μm remaining, or 99μm total thickness. So 99 is used as the critical thickness in determining the Z-score = (99-mean) / sigma.

Bearing life is determined by L₁₀ (Life when 10 % of the population will fail). So using the Z-score, a Failure Distribution Function is available for the amount of data which falls below the critical thickness. If the standard deviation tightens, the normal distribution becomes narrower, and the distance from the critical thickness (Z-score) increases. So the curve for the failure distribution can be determined based on Eq. (2).

DATA ANALYSIS

Instead of differentiating between bearings and measurement location, the data can be analyzed as a larger number of samples for each start stop interval, and then a hazard plot can be formed. The data statistics are shown in Table 3 [2]. Here the Confidence Interval is based on the t-distribution and is shown in Eq. (1).

$$C.I. = t_{\alpha/2, n-1} \frac{s}{\sqrt{n}} \quad (1)$$

(For α = 5%,
 t = 1.75 when n = 16
 t = 1.89 when n = 8)

$$F(c) = 1 - e^{-(c/\theta)^b}$$

$$\ln\{-\ln(1 - F(c))\} = -b \ln \theta + b \ln(c) \quad (2)$$

$$\ln(1 + F) = F \text{ as } F \rightarrow 0$$

shows the derivation of the shape and scale parameters for the cumulative failure distribution. This results in Eq. (3).

$$F(\text{cycles}) = 1 - e^{-\left(\frac{\text{cycles}}{10,460,000}\right)^{12.19}} \quad (3)$$

Table 3. Failure Probability Data Set

Start Stops	Mean (x)	st. dev (s)	n	C.I.	mean	mean		Failure
cycles	μm	μm	#	μm	- 95%CI	+ 95% CI	Z score	Probability
1	123.0	1.22	16	0.5	122.5	123.6	-19.76	3.06E-87
125,000	121.3	2.72	8	1.8	119.5	123.1	-8.21	1.13E-16
263,808	121.4	2.14	8	1.4	120.0	122.9	-10.49	4.91E-26
391,796	120.7	2.33	8	1.6	119.1	122.2	-9.21	1.68E-20
803,613	118.5	2.76	8	1.9	116.7	120.4	-7.07	7.88E-13
1,013,003	118.1	2.45	8	1.6	116.5	119.7	-7.81	2.91E-15

The Z-score is calculated using a critical coating thickness. The coating thickness will vary, and so

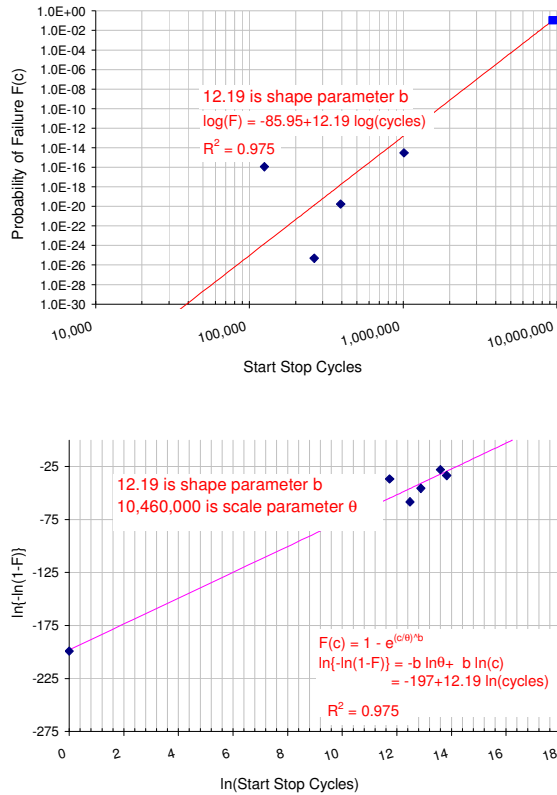


Figure 19. Cumulative Failure Distribution - Approx (top) and Exact (bottom)

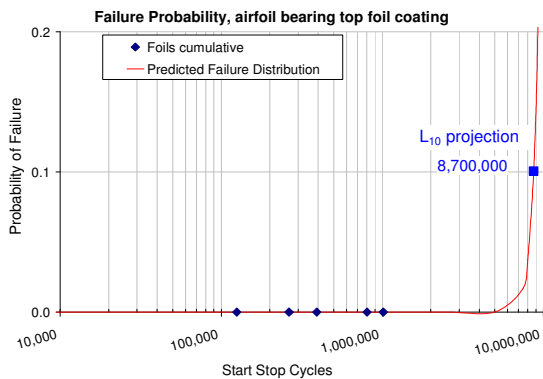


Figure 20. Failure distribution plot and predicted life

Figure 20 depicts a probability plot (Weibull) of the predicted top foil life, in number of start-stop cycles. This assumes a wear/loss of $2/3^{\text{rd}}$ of the top foil PTFE coating. The L_{10} value is 8.7 million start-stops.

CONCLUSION

On a final note, the lifetime of airfoil bearings for high speed continuous operation has no theoretical limit. While it is acknowledged that the rotor-foil system characteristic is an extremely important parameter affecting overall machine performance and life expectancy, a key concern for automotive applications has been the number of start up cycles as start-stop operation is generally much more prevalent in automotive environments. For high speed (75,000 rpm or greater) operation, the lifetime of the closest competitor technology, ceramic ball bearings, is less than 3,000 hrs. [2] This work examines the limiting factor of start-stop cycles on airfoil bearing lifetime in an automotive grade air compressor component.

The price increase for treating bearing journals with TiN and MoS_2 coatings is roughly 10 cents per journal in volumes of 100,000 or more per year. As for the stationary top foil, the additional cost for modifying the PTFE blend is insubstantial. Note the cost of the airfoil bearing set (front journals, aft journal, and thrust pad) is estimated to be roughly \$20 at those volumes. So for a 1% price change (2 journals per supercharger) the bearing life can be extended from 50,000 start-stops to over 1 million.

ACKNOWLEDGEMENTS

The authors would like to acknowledge the following individuals for contribution to this work. Todd Vancamp at Ford wrote the test stand software to test the hardware. Tony West at Ford provided 6-sigma statistical expertise in guiding the authors to the proper tools for data analysis. Chris Gearhart and Fred Brighton at Ford as well as Jim Middlebrook at Vortech provided management support to realize this project. Bill Bustamante and Jeff James at Vortech helped in the gauge selection to measure the bearings, as well as performed thickness measurements.

NOMENCLATURE

- AC Alternating Current
- ACM Air Cycle Machine
- BOL Beginning Of Life
- C.I. Confidence Interval
- DC Direct Current
- EOL End Of Life
- ESC Electronic SuperCharger
- F() Failure distribution function (Weibull probability density function)
- L_{10} Lifetime when 10% of population has failed
- PTFE Polytetrafluoroethylene or Teflon
- b Shape parameter, Weibull distribution

- n Number of samples
- s Standard deviation (of samples)
- t Test statistics (departure from mean) per standard normal distribution
- α Maximum acceptable probability that the effect is due to random variability in the data
- \emptyset Diameter
- θ Scale parameter, Weibull distribution

REFERENCES

[1] National Academies’ Committee on Alternatives and Strategies for Future Hydrogen Production and Use, 2009, *Hydrogen, Fuel Cells & Infrastructure Technologies Program Multi-Year Research, Development and Demonstration Plan*, US Department of Energy, pp. 3.4-3.22. <http://www1.eere.energy.gov/hydrogenandfuelcells/mypp/>

[2] Agrawal, G., 1997, "Foil Air/Gas Gearing Technology – An Overview," ASME Paper No. 97-GT-347. <http://www.rddynamics.com/foil-97-gt-347.pdf>

[3] Heshmat, H., and Hermal, P., 1993, "Compliant Foil Bearings Technology and Their Application to High Speed Turbomachinery," Elsevier Tribology International, **25**, pp. 559-575.

[4] Pinel, Signer, & Zaretsky, 1998, "Design and Operating Characteristics of High-Speed, Small-Bore, Angular-Contact Ball Bearings," NASA TM-1998-206981.

[5] DellaCorte, C., Zalana, A., and Radil, K., 2002, "A Systems Approach to the Solid Lubrication of Foil Air Bearings for Oil-Free Turbomachinery," NASA/TM -2002-11482.

[6] Heshmat, H., Hryniewicz, P., Walton II, J., Willis, J., Jahanmir, S., and DellaCorte, C., 2005 & 2006, "Low-friction wear-resistant coatings for high-temperature foil bearings," Elsevier Tribology International, **38(11-12)**, pp. 1059-1075.

[7] Pesaran, A., 2011, "Choices and Requirements of Batteries for EVs, HEVs, PHEVs," CALSTART Webinar, NREL/PR-5400-51474, pp. 38. <http://www.nrel.gov/vehiclesandfuels/energystorage/pdfs/51474.pdf>

[8] *Ford Confidential*. Kozarekar, Shailesh. Internal Memo "Analysis of Increase in Engine Start-Stops for GEN II Hybrid". Nov 2005.

[9] DellaCorte, C., and Valco, M. 2000, "Load Capacity Estimation of Foil Air Journal Bearings for Oil-Free Turbomachinery," NASA/TM -2000-209782.

[10] DellaCorte, C., and Radil, K., 2007, "Design, Fabrication and Performance of Open. Source Generation I and II Compliant. Hydrodynamic Gas Foil Bearings," NASA/TM—2007-214691.

[11] Engine Power Test Code, 1995, "Supercharger Testing Standard," SAE J1723.

TABLE OF TABLES

Table 1. Summary of ESC Bearing/Rotor System Parameters.....	3
Table 2. Measured Thickness, Journal Top Foils.....	7
Table 3. Failure Probability Data Set.....	8

TABLE OF FIGURES

Figure 1. Specific Power (kW/kg) and Power Density (kW/L) for candidate compressor technologies, taken at 2.5 PR and 325kg/hr air flow	1
Figure 2. Electronic Supercharger (ESC), Integral Motor/Compressor System	2
Figure 3. Airfoil Bearings	2
Figure 4. Assembled ESC Rotor System showing impeller (Left), fore/aft bearing journals, PM rotor, and thrust disk (Right).	3
Figure 5. Process diagram/schematic of test stand setup and operation.....	3
Figure 6. Test stand front view	3
Figure 7. 15s Start Stop profile.....	4
Figure 8. Top foil, baseline system, after 50k start-stops.....	5
Figure 9. Top Foil overall thickness measurement (left) and measurement locations (right).....	5
Figure 10. Gage R&R Graphical Results	6
Figure 11. Range Chart by Part.....	6
Figure 12. Start-stop run chart	6
Figure 13. 15s start-stop profile; speed	6
Figure 14. 15s Start-stop profile; air mass flow	6
Figure 15. Stop time and flow by Run	7
Figure 16. Stop time and flow by Date	7
Figure 17. Aft Top Foil, Progressive Wear	8
Figure 18. Aft Journal, Progressive Wear	8
Figure 19. Cumulative Failure Distribution - Approx (top) and Exact (bottom)	9
Figure 20. Failure distribution plot and predicted life.....	9